

Evolution of the optical properties of biomass-burning aerosol during the 2003 southeast Australian bushfires

Majed Radhi,¹ Michael A. Box,^{1,*} Gail P. Box,¹ Pawan Gupta,² and Sundar A. Christopher²

¹School of Physics, University of New South Wales, Sydney 2052, Australia

²Department of Atmospheric Sciences, The University of Alabama in Huntsville, Huntsville, Alabama, USA

*Corresponding author: m.box@unsw.edu.au

Received 3 July 2008; revised 12 November 2008; accepted 25 February 2009;
posted 26 February 2009 (Doc. ID 98319); published 17 March 2009

During January and February 2003, drought conditions led to major bushfires across southeast Australia, causing considerable damage. We have examined aerosol optical depth (AOD) data recorded by a sunphotometer at Wagga Wagga. Although this site lies to the northeast of the fires, periodic changes in wind direction brought smoke plumes over our instrument (AOD in excess of 1.0), sometimes via circuitous routes. By examining the hourly AOD spectra and, specifically, the Ångström exponent derived from our two shortest wavelengths, we have observed clear evidence of a shift in the peak radius of the fine mode, most likely as a result of particle coagulation. Selected data sets were inverted to obtain the aerosol size distribution, confirming this conclusion. This was particularly clear on 25 January, when the wind changed during the day so that the afternoon observations were of smoke that had traveled on a more circuitous route to the north of Wagga Wagga before returning. © 2009 Optical Society of America

OCIS codes: 010.1110, 010.1310, 010.0280, 010.5630.

1. Introduction

Fossil fuel and biomass burning are major sources of anthropogenic aerosol, with degradation of air quality and acid deposition linked to those sources. Several studies estimate the global scale of emission from biomass burning [1–6]. Ito and Penner [7] put the total emission from biomass burning at 2290 TgCyr^{-1} . They estimate that Australia is second in burned area, with $33.9 \times 10^6 \text{ ha yr}^{-1}$ after Sub-Saharan Africa, and contributes approximately 8% of global carbon emissions due to grassland, woodland, and forest burning.

Early in 2003, a series of devastating bushfires raged across large areas of the high country of southeast Australia. The prevailing winds, while predominantly from the west and north, carried smoke plumes in many directions, causing both local and regional effects. After a week of bushfires, the negative

radiative forcing over Canberra was -50 Wm^{-2} at the top of atmosphere and -172 Wm^{-2} at the surface [8], based on observations from a Cimel sunphotometer operated as part of CSIRO's Aerosol Ground Station Network (AGSNet), which is affiliated with NASA's AERONET. (These authors have also estimated the spectral single scattering albedo of the smoke.) This should be contrasted with Christopher *et al.* [9], who estimate instantaneous net radiative forcing for heavy biomass-burning aerosol over South America to be -36 Wm^{-2} .

In this paper we study the optical and physical properties of biomass-burning aerosol over Wagga Wagga, Australia (35.07°S , 147.23°E) during the bushfire period, based primarily on ground-based optical thickness data. The city of Wagga Wagga is the regional center of the rich agricultural and pastoral district of the Riverina in southern New South Wales, about 450 km southwest of Sydney and 180 km west of Canberra. The fires were approximately 100 to 200 km to the south and east of Wagga Wagga, so

that, for much of this time, the smoke plumes were largely carried away from this area.

However, on a number of occasions, some lasting for several days, winds brought considerable quantities of smoke aerosol to the atmosphere of Wagga Wagga. Because of the distance from the fires to Wagga Wagga and the sometimes indirect route taken by the smoke plumes, the smoke arriving here appears to have had time to age via such processes as condensation, coagulation, and gas-to-particle conversion [10]. This results in changes in the aerosol size distribution, which we have looked for in our optical thickness data.

Condensation involves the addition of volatile compounds to existing particles, resulting in an increase in mass and the growth in size of most particles. This will be reflected in an increase in optical thickness, and possibly a minor shift in its spectral dependence. By contrast, coagulation involves the collisional combining of smaller particles to form a smaller number of larger (accumulation mode) particles, without any increase in mass. This is also likely to lead to an increase in optical thickness, as the resulting larger particles will now be closer to the radius range of high mass extinction efficiency. In addition, the spectral dependence will clearly be changed at the short wavelength end. Such changes in fine-mode particle radius can occur with timescales varying from hours to days [10]. Coagulation is also more likely when smoke concentrations are higher.

In Section 2 we provide background information on our key data and methods of analysis, and also a summary of background aerosol optical properties in the region. In Section 3 we examine both radiometry and satellite data in order to obtain a detailed picture of the biomass-burning aerosol over Wagga Wagga in January and February of 2003. In Section 4 we focus on two periods of particularly intense smoke, including wind direction information and size distribution retrievals, which provide clear evidence of particle growth as the smoke aged.

2. Background

A. Data and Methods

Minute-by-minute aerosol optical depth (AOD) data, τ , were collected by a Middleton SPO2 sunphotometer, mounted on an automatic solar tracker with active Sun tracking. The tracking sensor ensures Sun alignment within 0.02° when the Sun is seen with four 25 mm diameter interference filters. The filters have 10 nm full width at half-maximum transmission centered at the nominal wavelengths of 412, 500, 610, and 778 nm, and four Hamamatsu silicon photodiodes. The sunphotometer measures the direct solar radiation. AOD is calculated based on the Beer–Lambert–Bouguer law. Calibration procedures and processing methods are described in Mitchell and Forgan [11]. In this study we will primarily be using τ at 500 nm as our measure of aerosol column loading.

The Ångström exponent, α , is computed from AOD measurements via a linear regression of $\ln \tau$ versus $\ln \lambda$. Ångström exponent values are used to give a qualitative idea of aerosol size distribution, with smaller values corresponding to large particle sizes (in general), and vice versa [12]. As the value of τ increases during a smoke episode, the value of α may sometimes be seen to decrease due to smoke ageing processes—coagulation, condensation [10]—leading to changes in the aerosol size distribution and, hence, the spectral dependence of AOD.

B. Long-Term Aerosol Optical Characteristics

In a previous work, Radhi *et al.* [13] investigated the seasonal variability of aerosol optical properties in the Wagga Wagga region for four years: 2001–2004. Here we provide a brief summary of that work, for completeness. The variability of daily average values of $\tau(\tau_D)$ during this period is presented in Fig. 1(a). This figure shows that τ_D rarely exceeds a background level of 0.1, while the monthly mean of AOD is generally less than 0.07, with some variation during summer months due to a combination of natural (biomass burning) and anthropogenic sources in that

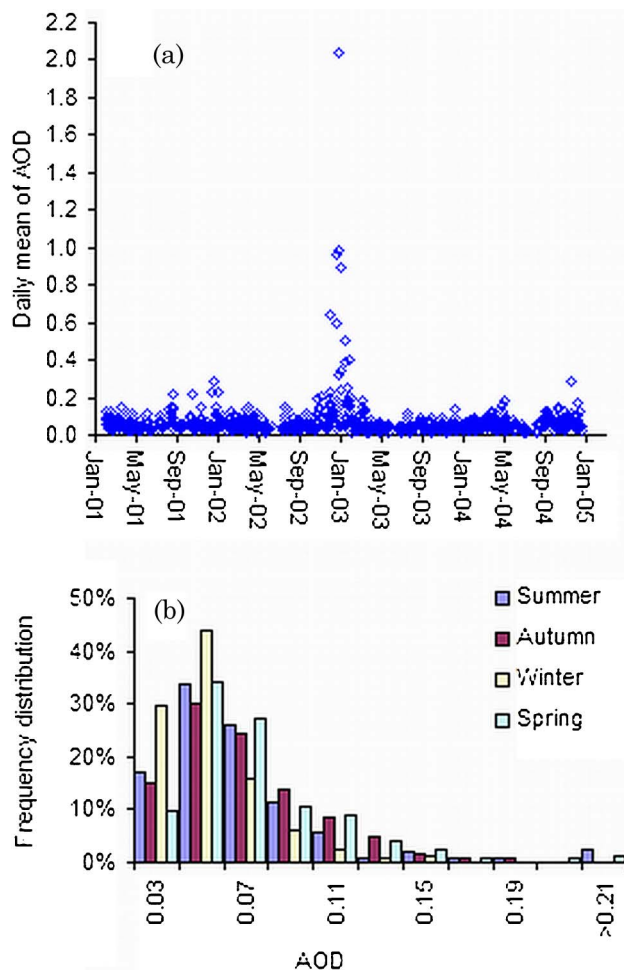


Fig. 1. (Color online) (a) Daily mean values of AOD at 500 nm, from March 2001 to December 2004, over Wagga Wagga. (b) Seasonal frequency distribution of daily means.

season [13]. The annual mean AOD computed from monthly averages is 0.06 ± 0.02 , which is lower than the lowest value estimated from the AERONET network, over Seville, New Mexico [14]. The seasonal frequency distribution for daily means of τ_D , presented in Fig. 1(b), shows that the probability distribution of τ_D is rather narrow, with a modal value of about 0.05, with approximately 80% of all observations during all seasons being less than 0.09, confirming a generally clean atmosphere over Wagga Wagga. An exception to these conditions occurred during the summer months of 2003: due to the southeast Australia bushfires that season, the value of τ_D exceeded 0.4 on a number of days, reaching as high as 2.0. These data were deliberately excluded from our earlier study, and form the basis of the current work.

The daily mean values of the Ångström exponent, α_F , which is obtained from a straight-line fit to $\ln \tau$ versus $\ln \lambda$ over the full wavelength range of 412 to 778 nm, showed large fluctuations day to day, with values ranging from about 0.25 to 2.0 (and occasionally beyond) due to the variety of aerosol types entering the surrounding atmosphere. The seasonal probability distribution of daily means of α_F , presented in Fig. 2, shows that approximately 50% of all observations are in the range of 1.0 to 1.6 (with an annual mean of 1.22, computed from the monthly means), which is a typical value assumed for mid-latitude rural conditions ([14]; see also [12]). The aerosol size spectrum would not appear to be strongly dominated by either coarse or fine-mode particles in Wagga Wagga during the period of study.

3. Aerosol Optical Properties during the 2003 Southeast Australia Bushfires

During January and February 2003 there was a number of large bushfires in southeast Australia that emitted significant quantities of smoke into the atmosphere. Biomass burning aerosol was advected in many directions, as shown in satellite images (Fig. 3). We have examined a range of data sources

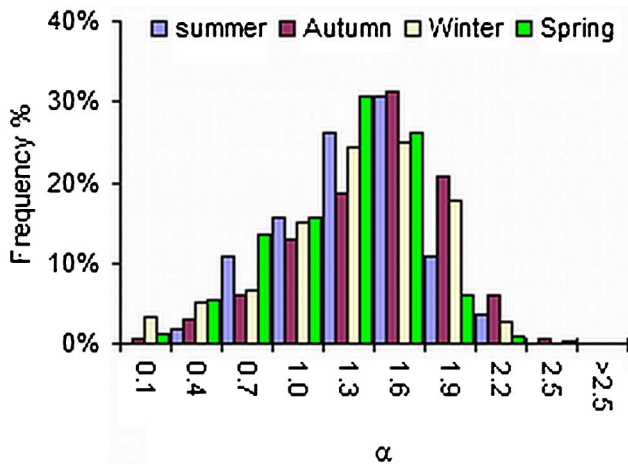


Fig. 2. (Color online) Seasonal frequency distribution of daily mean values of Angstrom coefficient α , from March 2001 to December 2004, over Wagga Wagga.

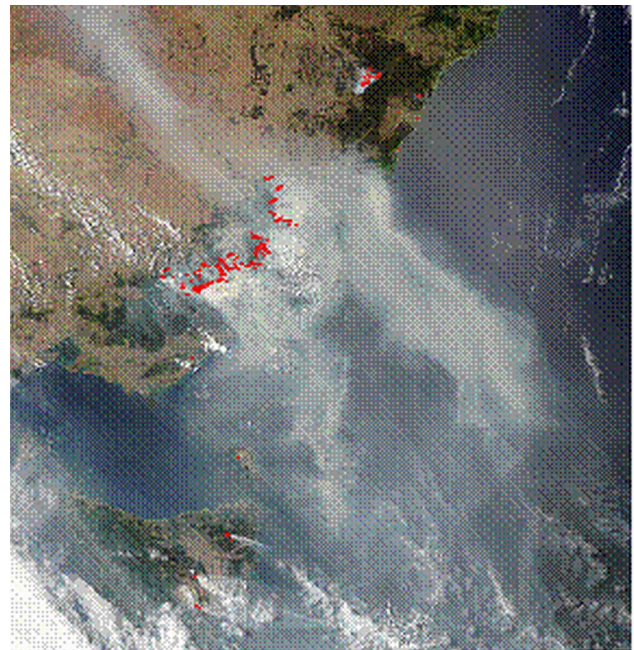


Fig. 3. (Color online) Plumes of smoke traveling to both the southeast and the northwest on 25 January 2003. (Image from Aqua at 03:35 UTC.)

in order to develop a detailed picture of the properties of this smoke and how it may have evolved over time. However, it is the (optical) remote sensing data which is of greatest value, due to its continuity throughout cloud-free periods.

A. Aerosol Optical Depth

Hourly average values of AOD, τ_H , were variable during this period, both day to day and during the day, exceeding 1.5 on some days; see Fig. 4. The monthly means of AOD during these months were around 3 times larger than for the same months during 2002 and 2004 (relatively smoke free); see Table 1. Further, approximately 60% of the daily averages of τ_D during the bushfire period (summer 2003) are greater than 0.09, in contrast to 80% of values less than 0.09 for the summer season background distributions (Subsection 2.B). This indicates the significant effect of biomass-burning aerosol during summer 2003 on the Wagga Wagga atmosphere.

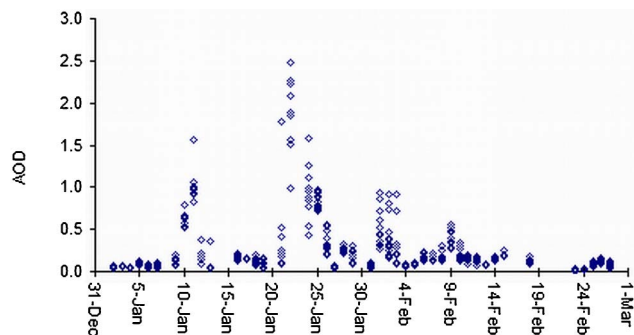


Fig. 4. (Color online) Hourly mean values of AOD over Wagga Wagga during summer 2003 southeastern Australia bushfires.

Table 1. Summary of Statistics of Aerosol Optical Properties during the Bushfire Months in 2003 and the Same Months for 2002 and 2004 (Relatively Smoke Free)

Date	AOD				Ångstrom Exponent			
	Mean	SD	Max	Min	Mean	SD	Max	Min
Jan. 02	0.09	0.08	0.29	0.02	1.37	0.45	2.06	0.43
Feb. 02	0.05	0.03	0.11	0.02	1.32	0.31	1.67	0.42
Jan. 03	0.33	0.47	2.04	0.04	1.30	0.49	2.19	0.44
Feb. 03	0.17	0.12	0.50	0.02	1.15	0.37	1.85	0.32
Jan. 04	0.05	0.02	0.07	0.02	1.13	0.39	2.02	0.47
Feb. 04	0.05	0.02	0.09	0.02	1.27	0.31	1.85	0.54

We may also note from Fig. 4 that the variability of AOD during this period is not random but is, rather, episodic. This reflects the variations in prevailing wind direction in the region, in response to the changing synoptic situation over southeast Australia, which is characterized by the passage of high pressure cells and occasional fronts to the south of the continent.

B. Satellite Observation

The MODIS instruments on both the Terra and Aqua satellites measure the optical characteristics of the atmosphere, at approximately 10:30 a.m. and 1:30 p.m. local time, respectively. One of the products supplied by NASA is aerosol optical thickness at 550 nm. Figure 5(a) is a satellite image for 24 January, which shows considerable smoke along much of the southeast coastal area of Australia, including to the northeast of Wagga Wagga. Figure 5(b) shows the corresponding retrieved aerosol optical thickness for smoky regions.

We have compared the available satellite data with our ground-based observations for the bushfire period. (Ground-based observations, τ_{500} , were time averaged over a period of plus/minus 30 min of the satellite overpass time.) In Fig. 6(a) we present the time series for Terra, along with that for our ground-based observations, for January and February; the agreement is clearly significant. In Fig. 6(b) we present a scatter plot and regression line between the ground-based and space-based data sets, which confirm this agreement ($R^2 = 0.87$), apart from a (relatively) small offset of 0.15. Figs. 6(c) and 6(d) present a similar treatment of the Aqua data (for January only). Again the agreement is good, although the correlation coefficient ($R^2 = 0.77$) is reduced (and the offset increased), at least partly as a result of the reduced data quantity.

C. Ångstrom Exponents

While the standard Ångstrom exponent is an important single parameter indicative of the aerosol size distribution [12], the aerosol optical depth spectrum contains more information than just a single parameter. Ångstrom exponent values computed from shorter wavelengths are known to be more sensitive to fine-mode particles than values computed from longer wavelengths [15,16]. We have computed the hourly average values of Ångstrom exponents from

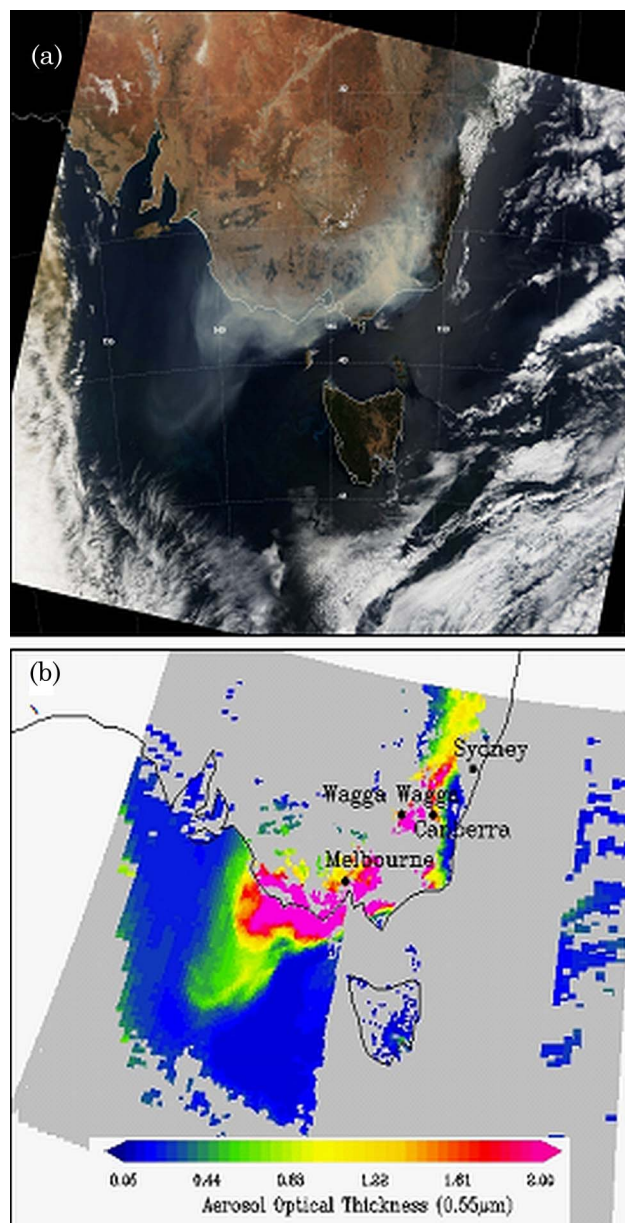


Fig. 5. (Color online) (a) Three-band (r, g, b) overlay of MODIS-Terra image on 24 January 2003, 0020 UTC, showing smoke plumes over Wagga Wagga and surrounding areas. (b) Aerosol optical thickness retrieval for the same image, showing very high AOD values (>2.0) for thick smoke plumes.

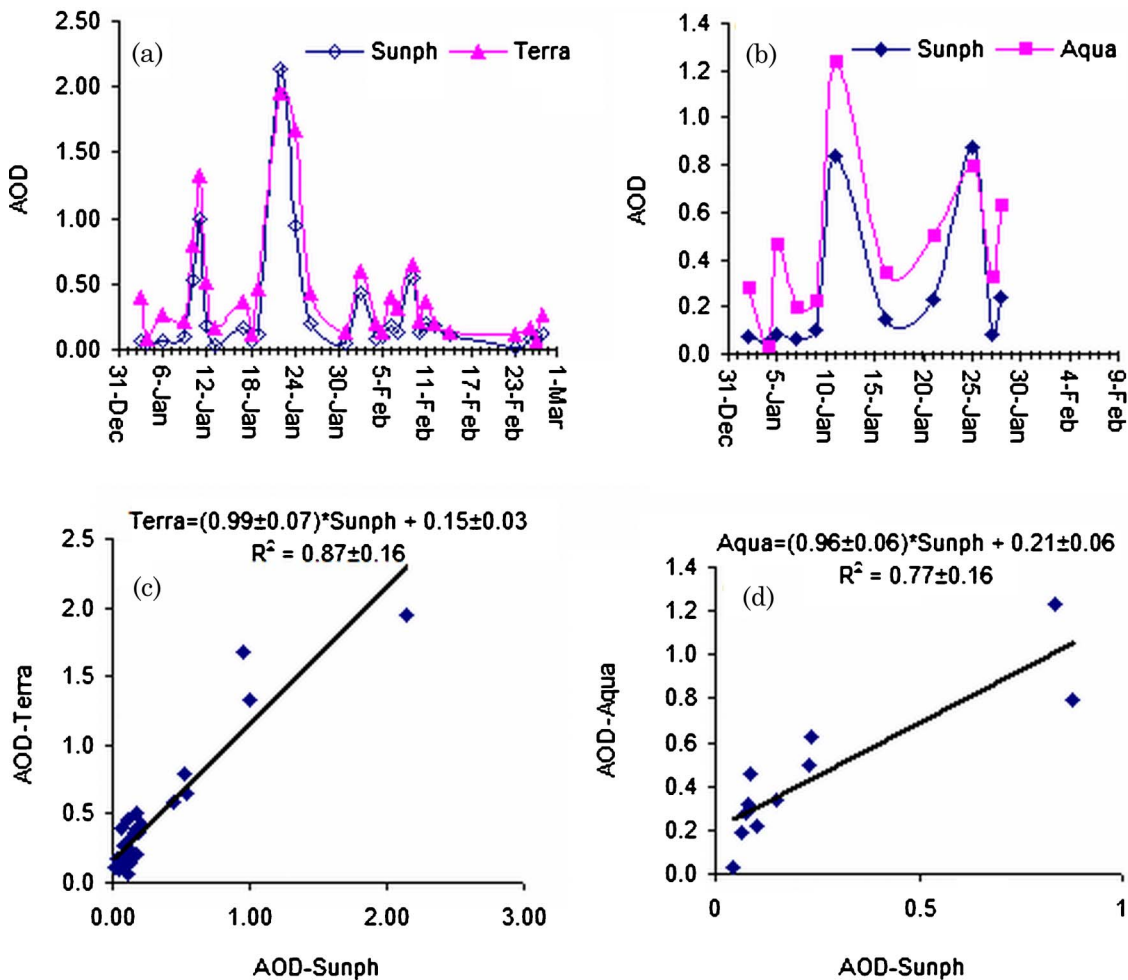


Fig. 6. (Color online) (a) Time series of AOD from ground-based (sunphotometer) and space-based (MODIS-Terra), during January and February 2003. (b) Scatter plot regression between the ground-based (sunphotometer) and space-based (MODIS-Terra) AOD, for the same period. (c) Time series of AOD from ground-based (sunphotometer) and space-based (MODIS-Aqua), during January 2003. (d) Scatter plot regression between the ground-based (sunphotometer) and space-based (MODIS-Aqua) AOD, for the same period.

the shorter wavelength pair, 412 and 500 nm (α_S); the longer wavelength pair (α_L), 610 and 778 nm; as well as the full wavelength set (α_F).

Figure 7 presents scatter plots of hourly average values of τ_H versus both α_S [Fig. 7(a)] and α_L [Fig. 7(b)]. These figures suggest that the data can be broken into two regions. The first is the background/smoke-affected region, with τ_H less than about 0.4; in this region α varies widely, implying a range of different types of aerosol from fresh smoke (fine-mode particles) to coarse-mode dust (caused primarily by agricultural activity). The region above about 0.4 is smoke dominated. Two features within this region are of interest. First, the data seems to fall into two groups: one with slightly higher α values, mainly from 10 to 12 January (circled); and the rest with slightly lower α values, from late January. This may well reflect differences in fire intensity and fuel type in these two time periods. (As well as native eucalypts, the later fires also involved pine plantations [8].)

Second we note that, on average, α_S values decrease as τ_H increases (at least for AOD below about

1.2), while the α_L values appear to increase as τ_H increases. There are two possible explanations for this, and probably both contribute. First, we may regard the aerosol in the Wagga Wagga atmosphere as a mixture of two components: the first of these is a background/dust aerosol, with relatively coarse-mode particles, while the second is the fine-mode smoke. Since it is clearly the smoke aerosol which is the major contributor in this region, its influence on the optical properties will tend to dominate the higher aerosol optical depth data. The second explanation relates to smoke aging. The α value often decreases as the AOD increases in smoky situations, due to the growth in size of the fine-mode particles, resulting from smoke aging processes—coagulation and condensation [10]. Optical depth increases as the particles become more efficient light scatterers, even though (at least in the case of coagulation) aerosol mass may not have increased.

4. Study of Two Intense Smoke Periods

Figure 4 shows two periods of very high AOD in January (9 to 12, and 22 to 25), as well as a period

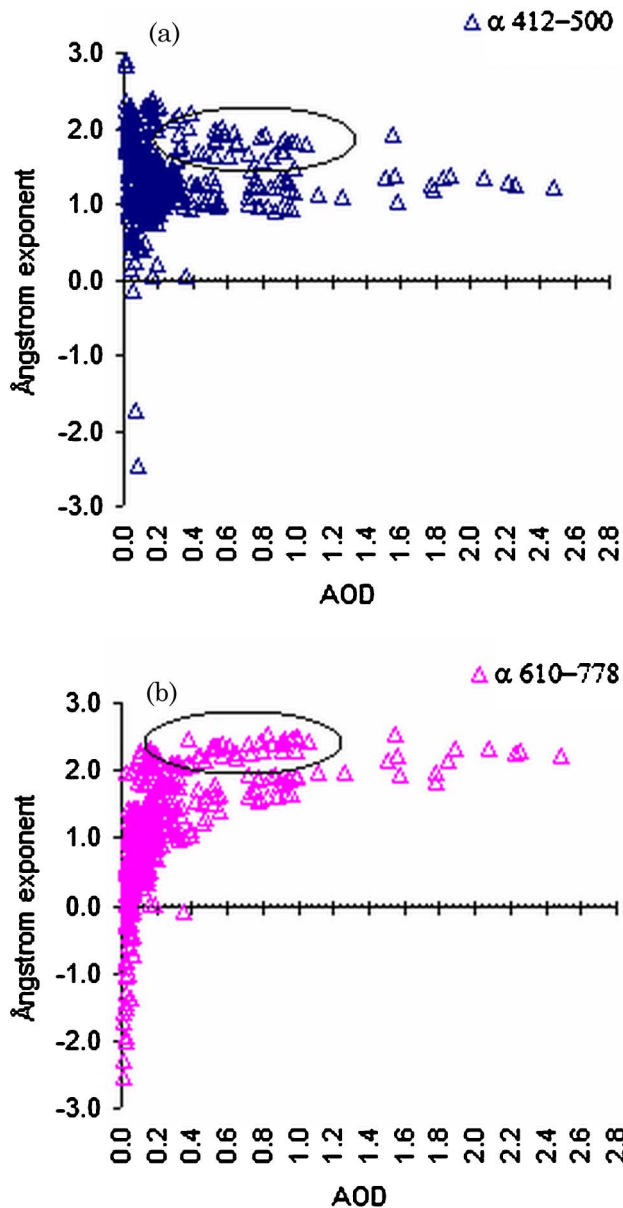


Fig. 7. (Color online) Scatter plot of hourly means of AOD versus both (a) α_S and (b) α_L .

in early February, when prevailing winds brought large amounts of smoke to the study area. We have examined the two January periods in greater depth, and now present an analysis of those results.

A. Aerosol Optical Properties During the First Intense Period

The AOD started to significantly exceed the background level (which we may take to be 0.1) on 9 January 2003, rising to hourly values of between 0.5 and 1.5 on the 10th and 11th, before decreasing rapidly on the 12th, reaching background levels again on the 13th, as shown in Fig. 4. The reasons for those dramatic changes are primarily a change in wind direction, as observed from both surface winds and back trajectory analysis (not presented). On the 9th, 10th, and 11th (morning and earlier afternoon)

the wind caused advection from bushfire regions to the south and southeast to increase the biomass-burning aerosol load over Wagga Wagga. On the afternoon of the 11th the wind direction changed to the east, and later the northeast, from non-bushfire areas, which helped to reduce the amount of biomass-burning aerosol in the atmosphere on the 12th and 13th.

Scatter plots of τ_H versus both α_S and α_L for the 9th, 10th, 11th, and 12th are shown in Fig. 8. When fresh smoke (small particles) predominates, the regression slopes between τ_H and both α_S and α_L are expected to be positive; this is evident on both the 9th and the 12th. Note that, on both days, the AOD values were comparatively low, indicating only moderate amounts of smoke. However, as the smoke concentration increases, the average particle size may grow due to smoke aging processes, especially coagulation. In these circumstances, as discussed above, the slopes become negative; 10 and 11 January are good examples.

The volume-weighted size distributions derived from the daily average AOD spectra for 7 to 13 January are shown in Fig. 9. These were obtained by inverting the AOD data using the constrained linear inversion technique developed by King *et al.* [17]. Note that no error levels have been included. The major contributor to retrieval errors would be the limited spectral range of the AOD measurements. An information content analysis [18] suggested that these data contain one to two pieces of information, which we take to be the peak radius, and possibly its width. We will focus on the peak radius.

Figure 9 shows that, during background levels of AOD (7 and 13 January), the distributions are quite flat with small total volume, and have a wide range of particle radii, a reflection of the range of local sources and processes. By contrast, the distributions for 10 and 11 January, following the arrival of higher levels of biomass-burning aerosol, show significant growth, especially in the fine mode, with a clear increase in mode peak radius. The peak of the volume distribution on 11 January is shifted from a radius of $\sim 0.06 \mu\text{m}$ (or less) when $\tau_{500} \sim 0.14$, to $\sim 0.1 \mu\text{m}$ when $\tau_{500} \sim 0.96$. This is consistent with the decrease of α_S as the smoke aged, as discussed above. Moreover, the accumulation-mode particle volume also increases as the AOD increases. This growth in the particle radius is likely to be at least partially related to the smoke aging processes of coagulation and condensation [10].

Kotchenruther and Hobbs [19] indicate that hygroscopic growth for biomass-burning aerosol is small for relative humidity of less than 50%, and is quite low when compared to industrial aerosol. Haywood *et al.* [20] echoed that conclusion for biomass-burning aerosol during the SAFARI 2000 campaign. We can thus be confident that hygroscopic growth of smoke aerosol may be neglected over Wagga Wagga because the relative humidity is quite low during summer months (generally less than 50%), and especially

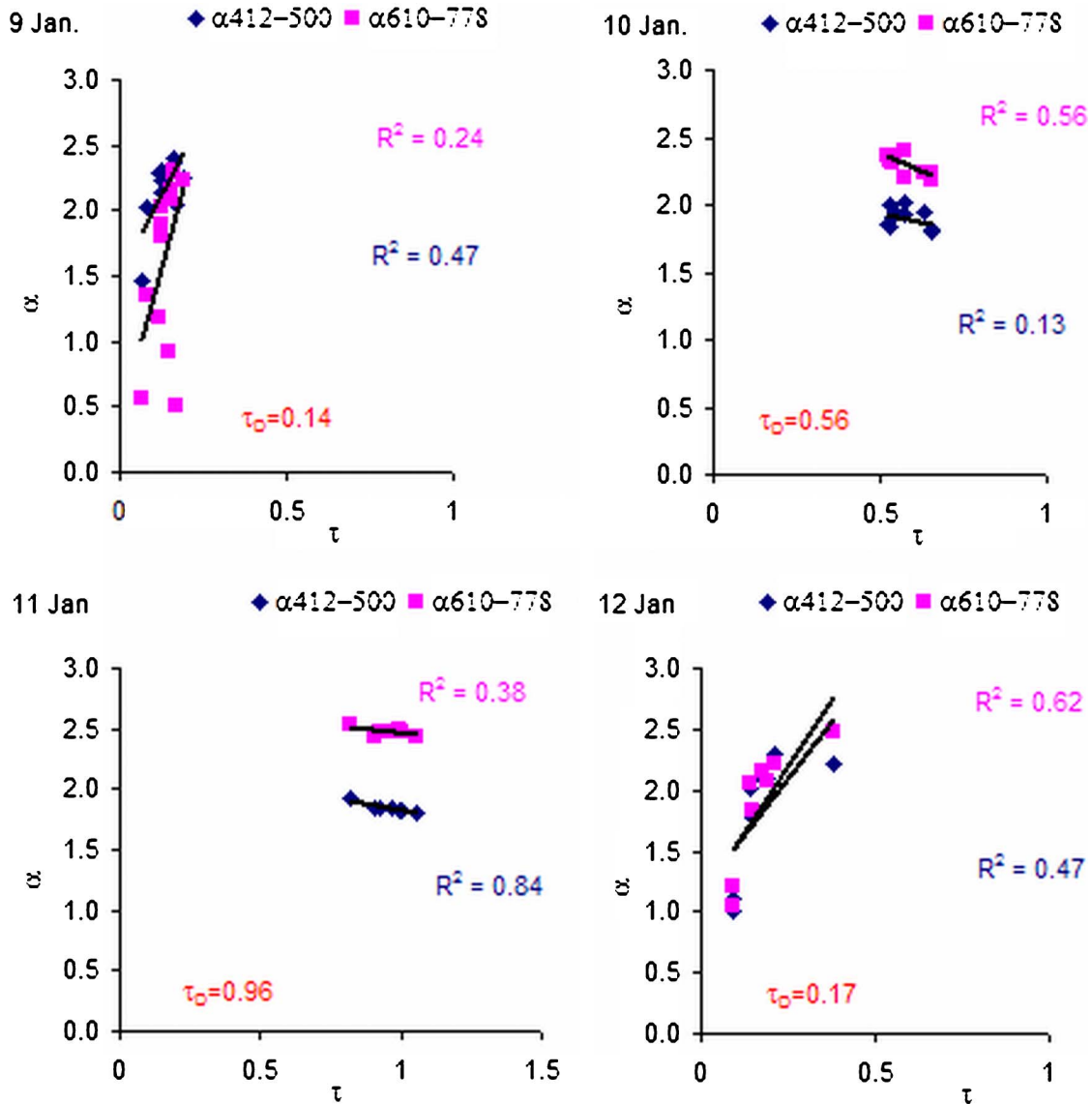


Fig. 8. (Color online) Scatter plots of τ_L versus both α_S and α_L for 9, 10, 11, and 12 January 2003.

so during bushfire periods. Hence, we may conclude that changes in the size distribution of the smoke aerosol over Wagga Wagga are a result of either advection or the smoke aging processes (or both).

B. Aerosol Optical Properties during the Second Intense Period

During mid-January, fires around Canberra (150 km east of Wagga Wagga) became intense and destructive [8], with winds mainly from the west. After the winds changed to bring more smoke to Wagga Wagga, the period from 22 to 25 January saw τ_D values range from 1.0 to 2.0, with some τ_H values reaching 2.5. January 25 proved to be a particularly interesting day. A scatter plot of τ_H versus both α_S and α_L on that day shows that the measurements seem to fall into two groups; see Fig. 10(a). When we divided the measurements into morning (6 a.m.–12 noon) and afternoon (1–6 p.m.) periods [Figs. 10(b) and 10(c), respectively] we found that the regression

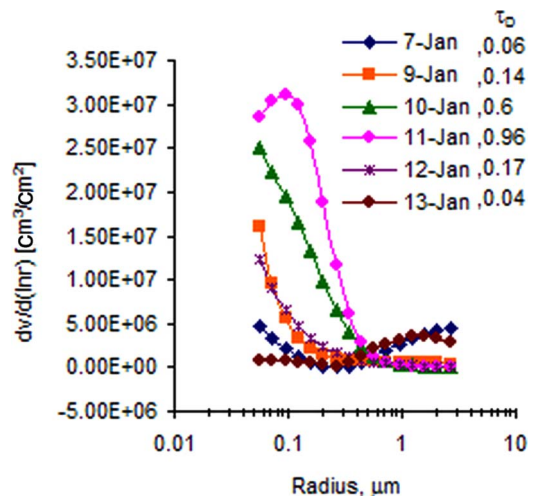


Fig. 9. (Color online) Particle volume-weighted size distributions from 7–13 January 2003.

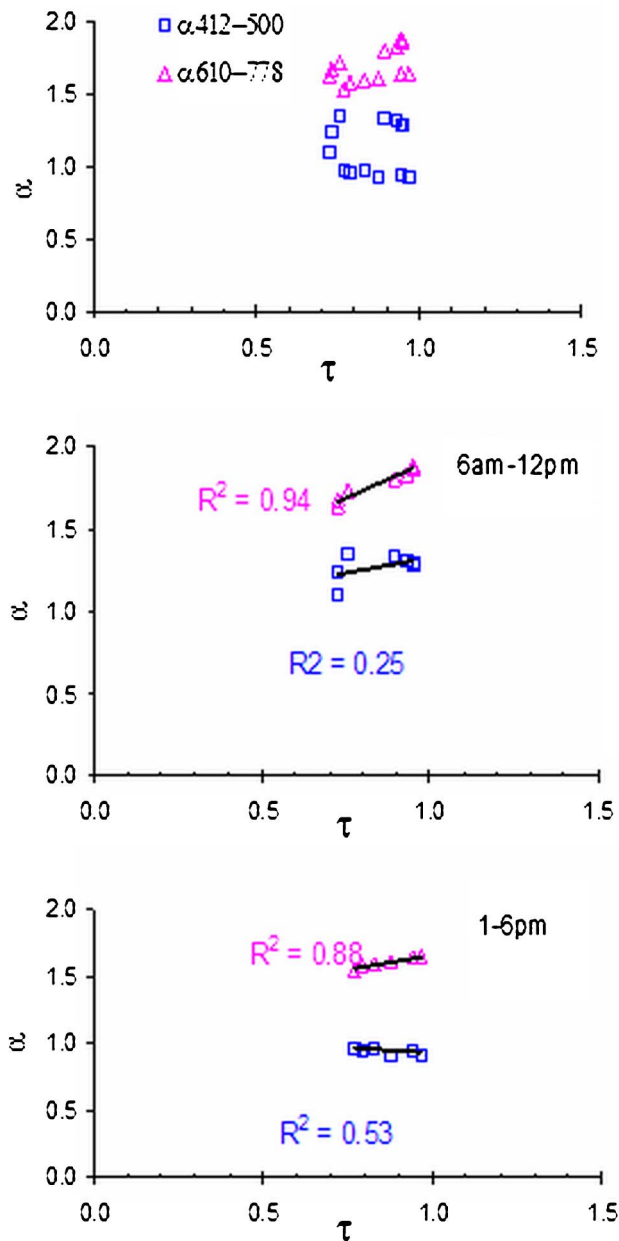


Fig. 10. (Color online) Scatter plots of τ_H versus both α_S and α_L on 25 January: (a) whole day, (b) morning period, and (c) afternoon period.

slope between τ_H and α_S is positive in the morning period and negative in the afternoon period. (The regression slope against α_L remained positive, although it decreased significantly.)

During the morning of 25 January, wind direction changed from east to north. We therefore studied back trajectories for a range of altitudes and times of arrival at Wagga Wagga. These showed that the smoke plume took a somewhat indirect route from the main source region to Wagga Wagga, first traveling to the northeast, in the direction of Sydney, before making a semicircular left turn and returning to the Wagga Wagga area (see also Fig. 5). This path actually increased in duration later in the day. As smoke

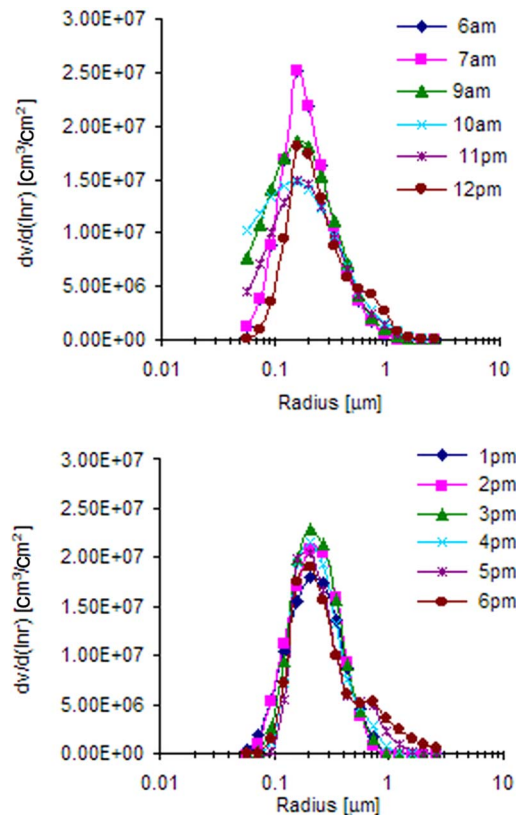


Fig. 11. (Color online) Hourly particle volume-weighted distributions during 25 January 2003: (a) morning and (b) afternoon.

aging is clearly a time-dependent process [10], the smoke aerosols which arrived in the afternoon are likely to be more aged, as a result of processes occurring along the way.

Figure 11 shows the hourly particle volume-weighted size distributions during 25 January. This figure shows a clear distinction between morning [Fig. 11(a)] and afternoon [Fig. 11(b)] size distributions, with a variation of $0.04 \mu\text{m}$ in the peak volume radius. (Note that Mitchell *et al.* [8] also provide size distribution retrievals over Canberra for the period of 17 to 25 January, based on AGSNet data. Their results, based on observations close to the source of the smoke plume, are broadly consistent with our retrievals in the accumulation mode, while providing additional information on the coarse mode.) In the morning the fine-mode particle volume peak was of a radius of $\sim 0.16 \mu\text{m}$ while, in the afternoon, the peak shifted toward a radius of $\sim 0.2 \mu\text{m}$ as a result of smoke aging. It is worth noting that, while τ_H was roughly in the same range for morning and afternoon, the values of α_S decreased as the smoke aged (particle radius increased); see Table 2. This further demonstrates the sensitivity of α_S to fine-mode particle size.

An inspection of Figs. 9 and 11 shows that the size distributions in this second period have higher peak radii than the first period. This is consistent with our observations in Subsection 3.C that there are two populations in Fig. 7, corresponding to these two

Table 2. Hourly Mean Values of τ_{500} and α_S during 25 January 2003

Time	τ_{500}	α_S
6	0.95	1.29
7	0.95	1.27
8	0.93	1.31
9	0.89	1.33
10	0.76	1.34
11	0.73	1.23
12	0.73	1.09
13	0.83	0.97
14	0.94	0.94
15	0.97	0.92
16	0.88	0.92
17	0.79	0.96
18	0.77	0.96

periods. There are a number of possible reasons for this difference. First, the second period involved smoke from pine plantations [8] as well as native eucalypts. Second, the smoke plumes in the later period were thicker (AOD exceeded 2.0 on 22 January), which should encourage coagulation. Finally, as we have just noted, the smoke plume in the second period traveled on a rather more circuitous route before reaching Wagga Wagga, allowing more time for coagulation.

5. Discussion and Conclusion

Southeastern Australia is known to be strongly affected by the El Niño/La Niña cycle, which has led to several major droughts in the past century. These conditions have been responsible for a number of disastrous bushfire seasons involving considerable property loss as well as the loss of many lives. January and February 2003 was the most recent example, with fires raging from the high country of northeast Victoria, through the Australian Alps, and on to the outskirts of the national capital, Canberra [8]. The speed of advance caught authorities and residents there by surprise and resulted in several deaths.

Though clearly less traumatic, these fires also had atmospheric consequences, in the form of smoke aerosol [8]. We have examined some of the effects of biomass-burning aerosol advected from these bushfires on the atmospheric environment of Wagga Wagga, using a wide range of data sources: ground-based radiometry, satellite observation, and winds and back trajectories. Although this city is to the north, or west, of the fires, and hence mostly upwind, periodic changes in wind direction brought large quantities of smoke over Wagga Wagga, with AOD exceeding 1.0 (1 hr average) on several occasions.

The most interesting outcome of this work is the clear evidence of smoke aging, which could be seen during the two heavy smoke episodes we investigated. Over periods of hours to days, smoke particles may coagulate [10], resulting in an increase in the peak radius of the fine-mode size distribution. This shift may manifest itself in two ways in the aerosol

optical depth spectrum. First, as the larger particles are more efficient light scatterers, AOD will increase. Second, we may observe a change in the spectrum at short wavelengths (depending on the spectral range of the measurements).

We have examined this spectral shift using two approaches. First, we have studied the Ångström exponent derived from our two shortest wavelengths, α_S , as this is quick and easy to obtain with large data sets. Scatter plots of α_S against AOD showed a negative slope in some circumstances, consistent with smoke coagulation. This was especially clear on 10 and 11 January, and also on the afternoon of 25 January. To reinforce these conclusions, we inverted selected AOD data sets to obtain the aerosol (volume-weighted) size distributions; see Figs. 9 and 11. These inversions show clear evidence of a shift in the peak of the fine mode as a function of time. When back-trajectory information is also brought into the picture, we conclude that smoke that has taken longer to travel from fire regions to Wagga Wagga has had more time to coagulate, a key process in smoke aging.

The authors thank the Australian Bureau of Meteorology, and especially Bruce Forgan, for providing optical depth data. This paper has benefited in several ways as a result of suggestions by the referees. This work was supported by Australian Research Council grant DP0451400.

References

1. W. Seiler and P. J. Crutzen, "Estimates of gross and net fluxes of carbon between the biosphere and the atmosphere from biomass burning," *Clim. Change* **2**, 207–247 (1980).
2. M. O. Andreae, "Biomass burning: its history, use, and distribution and its impact on environmental quality and global climate," in *Global Biomass Burning, Atmospheric, Climatic, and Biospheric Implications*, J. S. Levine, ed. (MIT Press, 1991), pp. 3–21.
3. W. M. Hao and M.-H. Liu, "Spatial and temporal distribution of tropical biomass burning," *Global Biogeochem. Cycles* **8**, 95–503 (1994).
4. C. Lioussé, J. E. Penner, C. Chuang, J. J. Walton, H. Eddleman, and H. Cachier, "A global three-dimensional model study of carbonaceous aerosols," *J. Geophys. Res.* **101**, 19411–19432 (1996).
5. J. M. Lobert, W. C. Keene, L. A. Logan, and R. Yevich, "Global chlorine emissions from biomass burning: reactive chlorine emissions inventory," *J. Geophys. Res.* **104**, 8373–8389 (1999).
6. G. R. van der Werf, J. T. Randerson, G. J. Collatz, and L. Giglio, "Carbon emissions from fires in tropical and subtropical ecosystems," *Global Change Biol.* **9**, 547–562 (2003).
7. A. Ito and J. E. Penner, "Global estimates of biomass burning emissions based on satellite imagery for the year 2000," *J. Geophys. Res.* **109**, D14S05 (2004).
8. R. M. Mitchell, D. M. O'Brien, and S. K. Campbell, "Characteristics and radiative impact of the aerosol generated by the Canberra firestorm of January 2003," *J. Geophys. Res.* **111**, D02204 (2006).
9. S. A. Christopher, D. V. Kliche, J. Chou, and R. M. Welch, "First estimates of the radiative forcing of aerosols generated from biomass burning using satellite data," *J. Geophys. Res.* **101**, 21265–21273 (1996).

10. J. S. Reid, P. V. Hobbs, R. J. Ferek, D. R. Blake, J. V. Martrins, M. R. Dunlap, and C. Lioussé, "Physical, chemical, and optical properties of regional hazes dominated by smoke in Brazil," *J. Geophys. Res.* **103**, 32059–32080 (1998).
11. R. M. Mitchell and B. W. Forgan, "Aerosol measurement in the Australian outback: intercomparison of sun photometers," *J. Atmos. Ocean. Technol.* **20**, 54–66 (2003).
12. H. D. Kambezidis and D. G. Kaskaoutis, "Aerosol climatology over four AERONET sites: an overview," *Atmos. Environ.* **42**, 1892–1906 (2008).
13. M. Radhi, M. A. Box, G. P. Box, and B. W. Forgan, "Seasonal cycles of aerosol optical properties at Wagga Wagga and Tennant Creek, Australia," *Clean Air Env. Qual.* **40**, 40–44 (2006).
14. B. N. Holben, D. Tanré, A. Smirnov, T. F. Eck, I. Slutsker, N. Abuhassan, W. W. Newcomb, J. S. Schafer, B. Chatenet, F. Lavenu, Y. J. Kaufman, J. Vande Castle, A. Setzer, B. Markham, D. Clark, R. Frouin, R. Halthore, A. Karneli, N. T. O'Neill, C. Pietras, R. T. Pinker, K. Voss, and G. Zibordi, "An emerging ground-based aerosol climatology: aerosol optical depth from AERONET," *J. Geophys. Res.* **106**, 12067–12097 (2001).
15. J. S. Reid, T. F. Eck, S. A. Christopher, P. V. Hobbs, and B. N. Holben, "Use of the Angstrom exponent to estimate the variability of optical and physical properties of aging smoke particles in Brazil," *J. Geophys. Res.* **104**, 27473–27489 (1999).
16. T. F. Eck, B. N. Holben, D. E. Ward, M. M. Mukelabai, O. Dubovik, A. Smirnov, J. S. Schafer, N. C. Hsu, S. J. Piketh, A. Queface, J. Le Roux, J. Swap, and I. Slutsker, "Variability of biomass burning aerosol optical characteristics in southern Africa during the SAFARI 2000 dry season campaign and a comparison of single scattering albedo estimates from radiometric measurements," *J. Geophys. Res.* **108**, 8477 (2003).
17. M. D. King, D. M. Byrne, B. M. Herman, J. A. Reagan, "Aerosol size distribution obtained by inversion of spectral optical depth measurements," *J. Atmos. Sci.* **35**, 2153–2167 (1978).
18. G. P. Box, M. A. Box, and J. Krucker, "Information content and wavelength selection for multispectral radiometers," *J. Geophys. Res.* **101**, 19211–19214 (1996).
19. R. A. Kotchenruther and P. V. Hobbs, "Humidification factors of aerosols from biomass burning in Brazil," *J. Geophys. Res.* **103**, 32081–32089 (1998).
20. J. Haywood, P. Francis, O. Dubovik, M. Glew, and B. Holben, "Comparison of aerosol size distributions, radiative properties, and optical depths determined by aircraft observations and Sun photometers during SAFARI 2000," *J. Geophys. Res.* **108**, 8471 (2003).